JOURNAL OF MATERIALS SCIENCE 25 (1990) 93–97

Crystallization of stable and metastable eutectics in FeSiB metallic glasses

M. A. GIBSON, G. W. DELAMORE
Department of Metallurgy and Materials Engineering, University of Wollongong, Wollongong, New South Wales 2500, Australia

Two iron-based metallic glasses, $Fe_{78}Si_9B_{13}$ and $Fe_{78}Si_{10}B_{12}$, have been examined after isothermal annealing at different temperatures and it has been found that both stable and metastable eutectics can crystallize simultaneously during the annealing process. At low temperatures, the majority of the eutectic cells in the structure consist of α-iron and the stable Fe_2B phase with a lesser amount of the α-iron and metastable Fe_3B eutectic, whereas at higher temperatures the metastable eutectic predominates. It is suggested that these observations may be explained in terms of the presence of overlapping coupled zones of both the stable and metastable eutectics in the phase diagram.

1. Introduction

The FeSiB metallic glasses are commercially important because they form the basis for the soft magnetic alloys currently being used for power transformer applications. Despite widespread investigation of these alloys, however, there still remain unresolved features of their crystallization behaviour which may be important in determining both the long-term stability of devices manufactured from them and also the extent to which their properties may be enhanced by controlled amounts of crystallization [1]. In particular, the fundamental question of the identity of the crystallization products in many of these alloys is still not completely resolved [2, 3] and recent work [4] has emphasized that it is unwise to assume that crystallization products forming at high temperatures will be the same as those resulting from lower temperature heat treatment.

Zaluska and Matyja [5] have shown that the structure of the primary phase crystallizing from a series of FeNiSiB glasses depends not only on the alloy but also, for any given composition, on the heating rate or the isothermal annealing temperature. We have also reported [6] that isothermal annealing of an $Fe_{75}Si_{10}B_{15}$ glass at two different temperatures resulted in an additional phase appearing in the microstructure at high temperatures and suggested that similar effects may be a feature of many metallic glasses but remain undetected because the annealing temperatures normally used for kinetic studies do not cover a sufficiently wide range.

The work reported here is part of a more detailed study of crystallization processes in FeSiB glasses. The eutectic product in at least two alloys in this system is shown to be dependent on annealing temperature.

2. Experimental work

10 g samples of $Fe_{78}Si_{10}B_{12}$ and $Fe_{78}Si_9B_{13}$ were prepared by melting together appropriate amounts of high-purity components in sealed quartz tubes under argon. The alloy buttons were subsequently homogenized by remelting several times on a water-cooled copper hearth in a small arc furnace. Ribbons approximately 5 mm wide and 25 to 30 μm thick were melt-spun in air on a stainless steel wheel, 300 mm diameter,

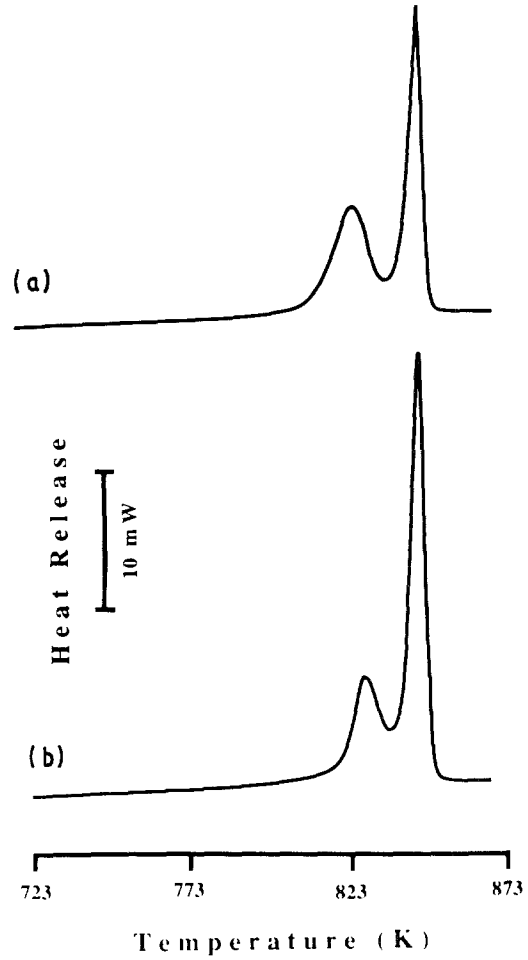

Figure 1 DSC thermograms at 20 K min^{-1}. (a) $Fe_{78}Si_{10}B_{12}$, (b) $Fe_{78}Si_9B_{13}$.

0022–2461/90 $03.00 + .12

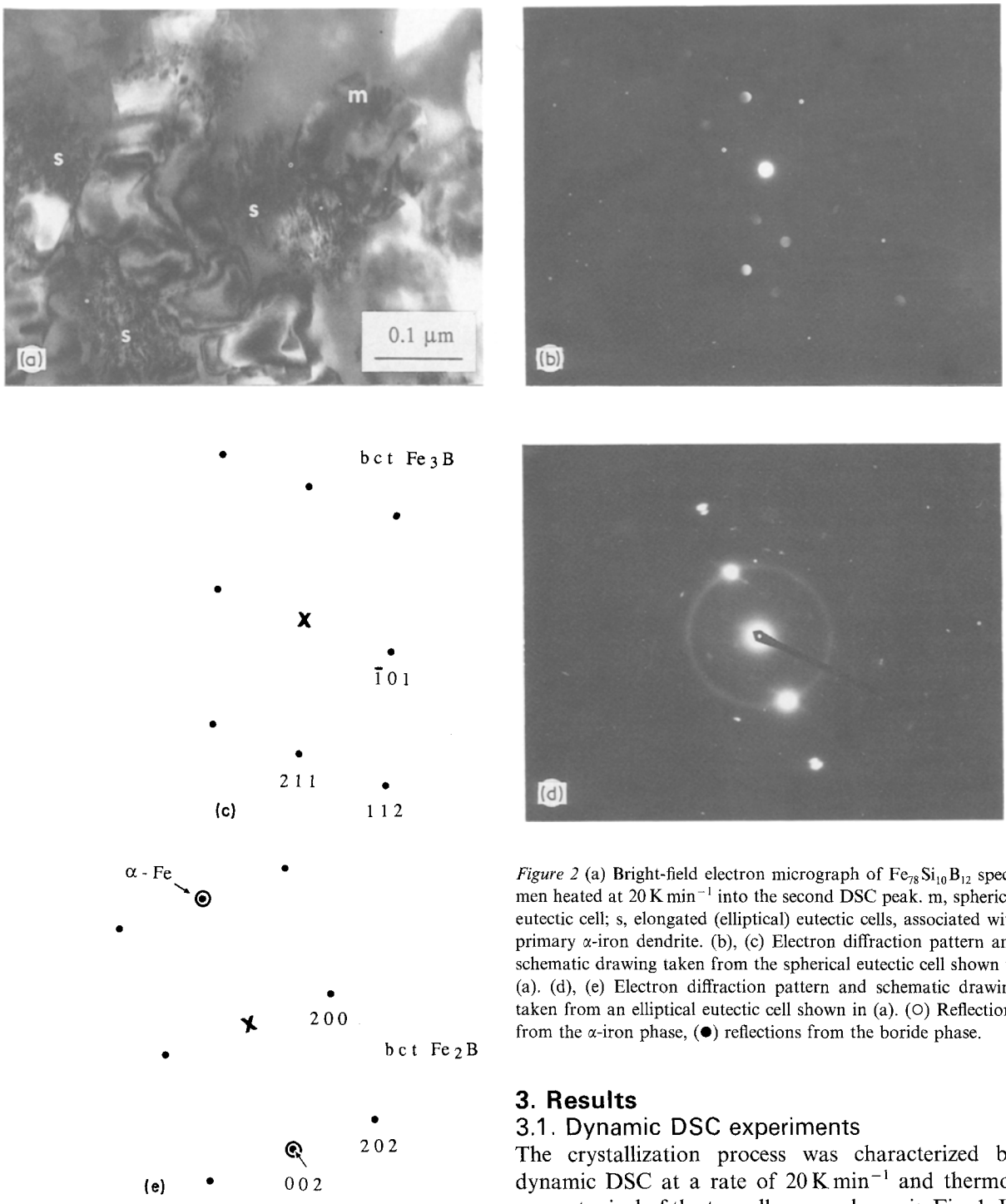

Figure 2 (a) Bright-field electron micrograph of $Fe_{78}Si_{10}B_{12}$ specimen heated at 20 K min^{-1} into the second DSC peak. m, spherical eutectic cell; s, elongated (elliptical) eutectic cells, associated with primary α-iron dendrite. (b), (c) Electron diffraction pattern and schematic drawing taken from the spherical eutectic cell shown in (a). (d), (e) Electron diffraction pattern and schematic drawing taken from an elliptical eutectic cell shown in (a). (○) Reflections from the α-iron phase, (●) reflections from the boride phase.

rotating at 2500 r.p.m. The ribbons were checked for lack of crystallinity by X-ray diffraction from both surfaces and by transmission electron microscopy (TEM), on electrochemically thinned foils. The ribbons were not analysed; the compositions given are nominal only.

Dynamic differential scanning calorimetry (DSC) using a Mettler TA 3000 system was used to characterize the crystallization behaviour of the alloys and to determine suitable temperature ranges for isothermal heat treatment. The isothermal annealing experiments were carried out in a lead bath on lengths of ribbon wrapped in aluminium foil and coated in colloidal graphite.

Partially-crystallized specimens were examined by TEM on foils prepared by electrochemical thinning in a Struers Tenupol twin-jet polisher.

3. Results

3.1. Dynamic DSC experiments

The crystallization process was characterized by dynamic DSC at a rate of 20 K min^{-1} and thermograms typical of the two alloys are shown in Fig. 1. In common with many other alloys in the FeSiB system, these thermograms are characterized by two peaks, the first associated with crystallization of a dendritic primary phase, in this case α-iron, and the second resulting from crystallization of a two-phase product. In both of the alloys examined, the peaks overlap to some extent making independent kinetic analysis of the peaks, as described in previous work [7], impossible. The microstructure of an $Fe_{78}Si_{10}B_{12}$ specimen, partially crystallized by interrupting a DSC run when into the second peak, is shown in Fig. 2a. Most of the two-phase product has the spherical overall morphology indicated in the figure but there are occasional regions where the eutectic cells have a more elliptical or elongated morphology and these regions are invariably closely associated with the primary dendrites as shown. The spherical eutectic cells outnumber the elliptical cells by a factor of approximately 50 to 1. An

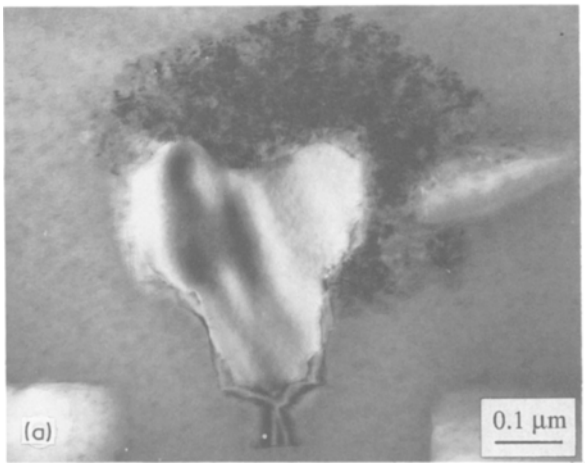

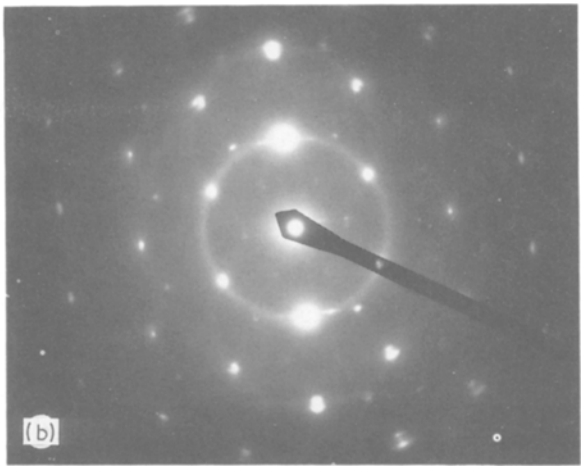

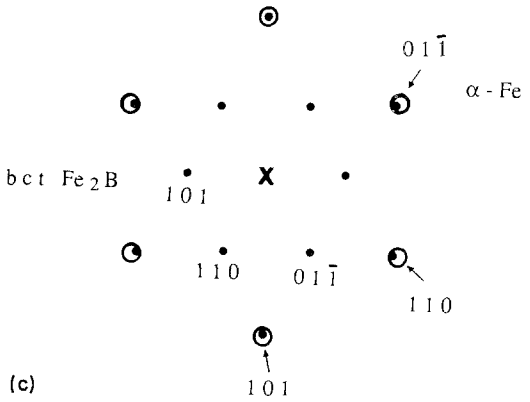

Figure 3 Bright-field electron micrograph of $Fe_{78}Si_{10}B_{12}$ annealed at 720 K for 45 h showing α-iron dendrite with associated α-iron/Fe_2B eutectic. (b), (c) Electron diffraction pattern and schematic drawing taken from a eutectic cell in (a). (○) Reflections from the α-iron phase, (●) reflections from the boride phase.

electron diffraction pattern taken of the spherical eutectic cell in Fig. 2a is shown in Fig. 2b. Analysis of this pattern indicates that the two-phase structure is composed of α-iron and Fe_3B. The diffraction pattern taken from the smaller, elliptical regions however, Fig. 2d, showed that the eutectic product in this case is α-iron and Fe_2B.

3.2. Isothermal heat treatment at 720 K

An electron micrograph illustrating the partially crystallized structure of the $Fe_{78}Si_{10}B_{12}$ alloy annealed at 720 K for 45 h is given in Fig. 3a. The primary crystallization product is identical with that produced by dynamic heat treatment at 20 K min^{-1}, namely well-formed dendrites of α-iron. The two-phase product has the elongated overall shape and fine, irregular internal morphology described above for the minority product in the dynamically heated samples: there was no evidence of the spherical eutectic cells. An electron diffraction pattern from a two-phase region is shown in Fig. 3b and is consistent with a eutectic product containing α-iron and Fe_2B. X-ray diffraction of partially crystallized specimens confirmed this analysis with no evidence of Fe_3B in the structure.

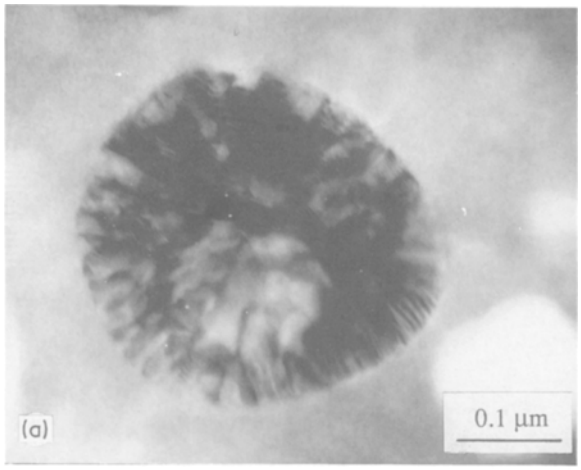

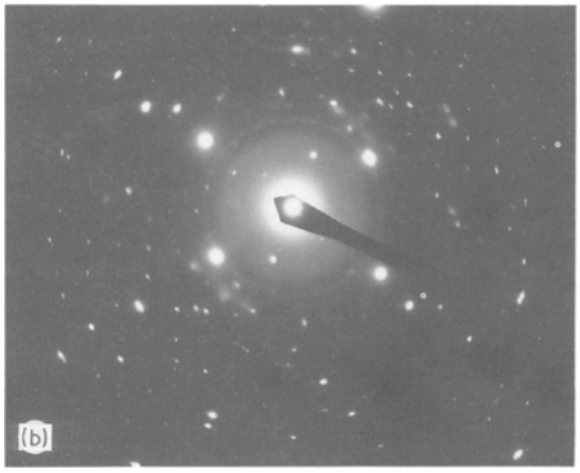

Figure 4 (a) Bright-field electron micrograph of $Fe_{78}Si_{10}B_{12}$ annealed at 773 K for 1 h showing a typical spherical eutectic cell containing α-iron and Fe_3B. (b), (c) Electron diffraction pattern and schematic drawing taken from eutectic cell in (a). (○) Reflections from the α-iron phase, (●) reflections from the boride phase.

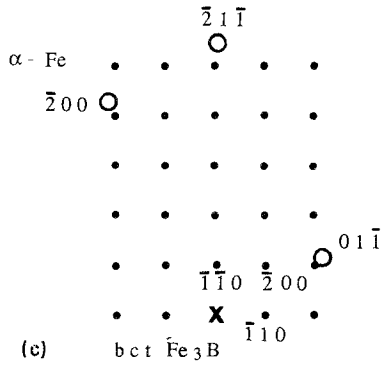

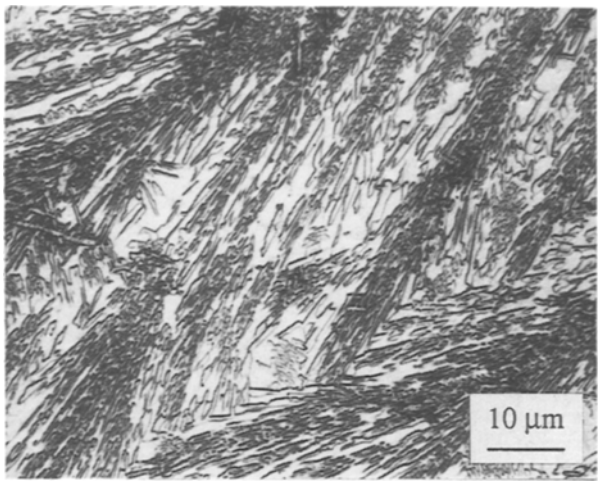

Figure 5 As-cast microstructure of $Fe_{78}Si_{10}B_{12}$ consisting almost entirely of eutectic Fe_2B and α-Fe.

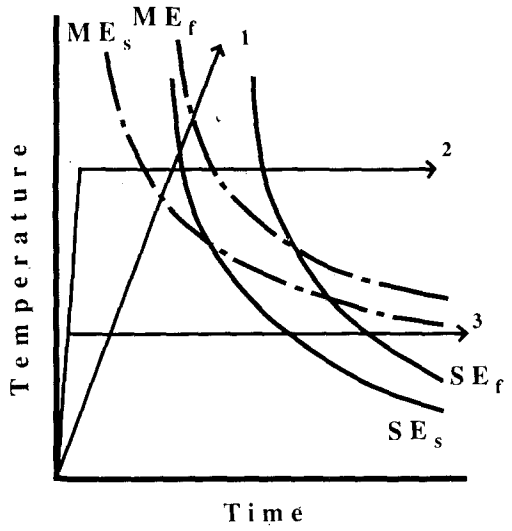

Figure 6 Schematic time–temperature–transformation diagram showing possible crystallization routes for the glass. ME_s and ME_f represent start and finish lines for the metastable eutectic between α-iron and Fe_3B: SE_s and SE_f are equivalent lines for the stable eutectic containing α-iron and Fe_2B. Superimposed lines indicate transformation paths for samples: (1) continuously heated; (2) isothermally annealed at high temperature; (3) isothermally annealed at low temperature.

3.3. Isothermal heat treatment at 773 K

Fig. 4a shows the microstructure of the $Fe_{78}Si_{10}B_{12}$ alloy after annealing at 773 K for 1 h. In this case the majority of the eutectic cells (~80%) have the general spherical overall shape with a distinctly lamellar internal structure and there is no obvious association of the cells with primary dendrites. An electron diffraction pattern taken from these cells (Fig. 4b) shows them to contain a mixture of α-iron and Fe_3B. The smaller proportion of the elongated eutectic product was again shown by electron diffraction to be α-Fe and Fe_2B. X-ray diffraction confirmed the presence of Fe_3B but Fe_2B could not be detected, presumably because the technique is insensitive to the relatively small amounts which are present in the structure.

The results for the $Fe_{78}Si_9B_{13}$ alloy were essentially the same as those for $Fe_{78}Si_{10}B_{12}$ at each annealing temperature and in the dynamic DSC experiments.

4. Discussion

The as-cast microstructure of the $Fe_{78}Si_{10}B_{12}$ alloy is shown in Fig. 5 and consists almost entirely of a eutectic of Fe(Si) and Fe_2B although there is a very small number of faceted crystals of primary Fe_2B in the structure. This microstructure and the phases present are consistent with published data on the FeSiB system [8] which indicates that the alloy composition is very close to a eutectic trough in the ternary diagram. Other alloys in the FeSiB system investigated previously [7] also suggest that the proposed phase diagram is accurate, at least in this composition range. The fact that the structure is virtually entirely eutectic when solidified from the melt whereas non-faceted α-iron dendrites form in the same alloy crystallized from the glass is evidence that a skewed coupled zone exists in this system, as proposed in earlier work [9], and this presumably reflects the growth difficulties associated with the faceting Fe_2B phase as compared to the primary α-iron dendrites.

The change in eutectic product with annealing temperature has not, to our knowledge, been reported in the literature on metallic glasses. It is, however, consistent with previous work suggesting that primary crystallization products in metallic glasses are a function of both heating rate and annealing temperature [5, 6]. It is also well-documented that some alloys can solidify to different eutectic products depending on cooling rate: for example, with increasing freezing rate the product in Al–Fe changes from the equilibrium Al–Al_3Fe eutectic to the metastable Al–Al_6Fe or Al–"S" phase eutectics [10, 11].

It seems clear that those processes that govern phase selection during freezing from the melt are also operating during crystallization of the glassy alloys. In the present case, the metastable eutectic between α-Fe and Fe_3B appears to exist over a range of compositions and temperatures when crystallized from the glass and this range forms a coupled zone in the metastable phase diagram which overlaps a similar coupled zone for the stable eutectic between α-Fe and Fe_2B. During isothermal annealing, either or both eutectic products may form, depending on temperature, as indicated schematically in Fig. 6. Similarly, dynamic heating may produce a mixture of both eutectics, the proportion of each depending on heating rate.

It is unlikely that simultaneous crystallization of the two eutectics is restricted to the alloys examined in this work, but for other compositions the relative positions of the two coupled zones will alter both the amounts of the two eutectic types in the structure and the heat-treatment temperatures at which each predominates. This may be the reason for the apparently limited range of compositions in the FeSiB system in which the metastable Fe_3B phase has been reported previously [2]. In addition, the difficulties asssociated with determining by X-ray diffraction alone the simultaneous presence of Fe_2B and Fe_3B when one of them is present in small amounts may also explain some of the confusion in the literature on the nature of the crystallization products in these alloys and emphasizes the need for complementary metallographic work in this type of study.

5. Conclusions

The eutectic product arising from the crystallization of at least some metallic glasses in the FeSiB system depends on the isothermal annealing temperature. At high temperatures, most of the eutectic cells in the structure consist of α-iron and Fe_3B whereas at lower temperatures this eutectic is largely replaced by one containing α-iron and the stable Fe_2B phase. This result is interpreted in terms of the existence of coupled zones of both the stable and metastable eutectics in the FeSiB system. It seems probable that similar combinations of stable and metastable crystallization products exist in other metallic glasses but remain undetected because of the limited range of heat-treatment temperatures normally used in experiments to determine crystallization kinetics.

Acknowledgement

We gratefully acknowledge financial support for this work from the Australian Research Council.

References

1. R. HASEGAWA, V. R. V. RAMANAN and G. E. FISH, *J. Appl. Phys.* **53** (1982) 2276.
2. A. ZALUSKA and H. MATYJA, *J. Mater. Sci.* **18** (1983) 2163.
3. A. QUIVY, J. RZEPSKI, J.-P. CHEVALIER and Y. CALVAYRAC, in Proceedings of the Fifth International Conference on Rapidly Quenched Metals, edited by S. Steeb and H. Warlimont, Warzburg, 1985 (Elsevier, Amsterdam, 1985) p. 315.
4. B. CANTOR, in "Amorphous Metals and Semiconductors", edited by P. Haasen and R. I. Jaffee, (Pergamon, New York, 1986) p. 108.
5. A. ZALUSKA and H. MATYJA, *Mater. Sci. Engng* **97** (1988) 347.
6. M. A. GIBSON and G. W. DELAMORE, *Mater. Sci. Tech.* **4** (1988) 700.
7. *Idem, J. Mater. Sci.* **22** (1987) 4550.
8. B. ARONSSON and I. ENGSTROM, *Acta Chem. Scand.* **14** (1960) 1403.
9. M. A. GIBSON and G. W. DELAMORE, *Mater. Sci. Engng* **101** (1988) 135.
10. I. R. HUGHES and H. JONES, *J. Mater. Sci.* **11** (1976) 1781.
11. D. SHEETMAN and L. J. SWARTZENDRUBER, in "Alloy Phase Diagrams", edited by L. H. Bennett, T. B. Massalski and B. C. Giessen, Materials Research Society Symposium Proceedings, Vol. 19 (Elsevier, New York, 1983) p. 265.

Received 26 September 1988
and accepted 27 February 1989